Exact calculation of the tortuosity in disordered linear pores in the Knudsen regime

Stefanie Russ
Institut für Theoretische Physik, Freie Universität Berlin, Arnimallee 14, 14195 Berlin, Germany
(Received 28 January 2009; revised manuscript received 10 November 2009; published 28 December 2009)

The squared reciprocal tortuosity $\kappa^{-2}=D/D_0$ for linear diffusion on lattices and in pores in the Knudsen regime is calculated analytically for a large variety of disordered systems. Here, D_0 and D are the self-diffusion coefficients of the smooth and the corresponding disordered system, respectively. To this end, a building-block principle is developed that composes the systems into substructures without cross correlations between them. It is shown how the solutions of the different building blocks can be combined to gain D/D_0 for pores of high complexity from the geometrical properties of the systems, i.e., from the volumes of the different substructures. As a test, numerical simulations are performed that agree perfectly with the theory.

DOI: 10.1103/PhysRevE.80.061133 PACS number(s): 05.40.Fb, 47.56.+r, 66.30.je

I. INTRODUCTION

Diffusion in random media has been a subject of large interest in the past decades (for some latest reports, see, e.g., [1]). In the last years, the interest has focused on the experimentally accessible subject of diffusion of gas molecules in pores (see Fig. 1), as, e.g., the human lung [2], linear silicon nanochannels [3] or zeolithes, and other micropore and nanopores [4–6]. As recent progress in synthesizing nanostructured porous materials has provided the options of designing specific pore architectures [7], an exact analytical understanding of the diffusion process is of great importance. Of particular interest is the tortuosity factor $\kappa=\sqrt{D_0/D}$ that describes the relation between the diffusion coefficients D and D_0 of systems with and without geometrical disorder [8]. Both D and D_0, can be gained by studying either the transport or the self-diffusion problem, where in the Knudsen regime, the self- and the transport diffusion coefficients are the same for a given geometry. Theoretical calculations of D on complex pores have mostly been based on numerical simulations of the transport [9–12] or the self-diffusion problem [11–15] and/or phenomenological or semianalytical approaches [16], whereas exact analytical results of specific pore geometries have only been provided along loopless curved one-dimensional paths [17] and for systems with dead ends [18,19]. In loopless curved systems [see Figs. 2(b) and 2(e)], the tortuosity factor is determined by the longer path, the particle has to travel along the curve in order to overcome a smaller distance in x direction, and the diffusion time of a particle in pores with dead ends [as shown in Figs. 2(c) and 2(f)] is increased by detours into the dead ends that do not contribute to the diffusion along the x direction.

The purpose of this work is to create an approach, based on the self-diffusional problem, for the exact analytical calculation of D/D_0 of more complex systems, as the ones in Fig. 2. To this end, we consider the lattice problem and its connection to diffusion in linear pores in the Knudsen regime [20] (see below). To calculate D/D_0, we decompose the considered complex systems (see Fig. 3, for examples) into simpler exactly solvable geometric substructures (building blocks) without cross correlations between them and show how the results of the single subunits must be combined to calculate D/D_0 as a function of simple geometrical data, i.e., of the different lengths, widths, and volumes, as given in Table II. We verify our results by numerical simulations that agree perfectly with the theoretical predictions. In this work, we are only interested in systems where a fully analytical treatment is possible, i.e., where all individual building blocks can be solved analytically. However, we would like to point out that this method can also go beyond these cases by combining analytical and numerical data of different building blocks.

The paper is organized as follows. In Sec. II, we present the random walk on a lattice and the diffusion problem in pores, while the underlying theory for the calculation of D for systems made of various building blocks is explained in Sec. III. In Sec. IV, we present the theoretical results and verify them by numerical simulations. In the last Sec. V, we discuss the results and give an outlook.

II. DIFFUSION ON LATTICES AND IN PORES

In a linear random walk, a particle jumps inside a d-dimensional lattice (see left column of Figs. 2 and 3) and we are interested in its displacement in x direction. We concentrate on problems, where despite an irregular structure of the systems the long-time diffusion stays normal, which means that D for long times is defined by the Einstein relation,

$$\lim_{t\to\infty}\langle x^2(t)\rangle = 2Dt, \tag{1}$$

where the mean-square displacement $\langle x^2(t)\rangle$ is the squared distance, a particle has traveled during time t in x direction. For anomalous diffusion, as, e.g., on fractal structures, we refer to the literature [21–24]. For simplicity, we concentrate on cubic (square) lattices, where in the absence of disorder

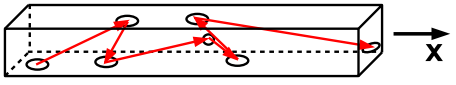

FIG. 1. (Color online) Sketch of the diffusion process inside a (smooth) pore. The particle is reflected with different angles between the pore walls, leading to jump lengths of very different sizes.

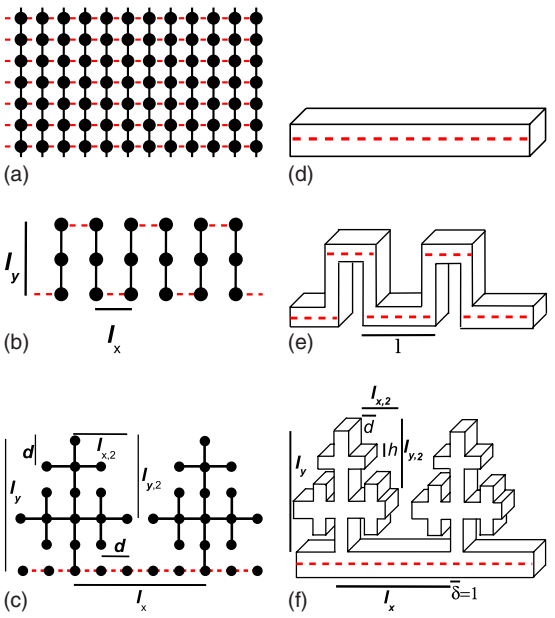

FIG. 2. (Color online) Sketch of the geometries of special well-known subunits for lattices [(a)–(c), left column] and the corresponding pores [(d)–(f), right column], i.e., regular units [(a) and (d)], curved units [(b) and (e)], and systems with dead-end units [(c) and (f)]. In the pores, all x channels (red dashed lines) are of square cross section (with side length h) and up to 1000 of these (identical) blocks are sticked together to account for an infinite elongation into the x direction. For further geometric details, see the caption of Table I.

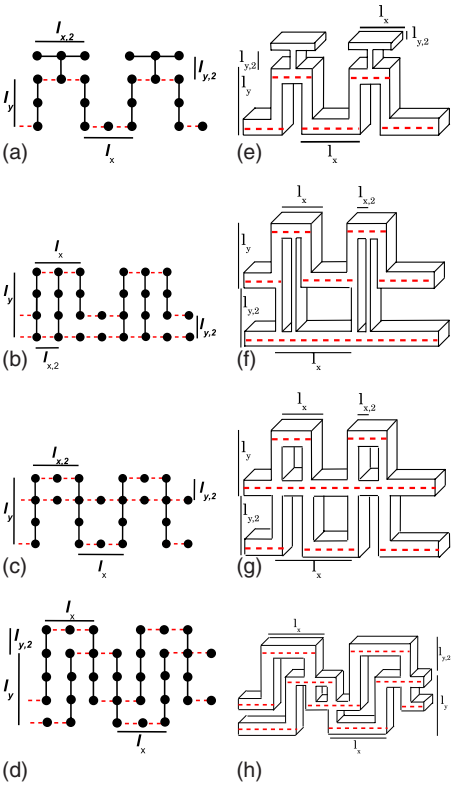

FIG. 3. (Color online) Geometries for lattices (left column) and the corresponding pores (right column) that are analyzed by the building-block principle: [(a) and (e)] curved system with dead ends, [(b) and (f)] curved system in parallel with a channel, [(c) and (g)] curved system intersected by a channel, and [(d) and (h)] system of two intersecting curves. All x channels (red dashed lines) of pores are of square cross section with side length h and up to 1000 of these (identical) blocks are sticked together to account for an infinite elongation into the x direction (for further geometric details, see Table II).

each lattice site has $2d$ neighbors and on unbiased walks, where jumps to the neighboring sites occur with equal probability. Disorder is created by the removal of sites or of links between neighboring sites. On a lattice, a walker chooses one of the $2d$ possible directions for the following jump at random. If the link to the chosen neighbor is existing, the walker jumps, thereby, performing a jump of length a (lattice constant) during a time step τ. If the link has been removed, the walker stays for this time step where it is (waiting time).

Diffusion in pores (right column of Figs. 2 and 3) represents a more complex problem where, in general, the track of the gas molecules through the pores depends on the collisions between the gas molecules as well as on the collisions of the gas with the pore walls. In cases where Knudsen diffusion [20] dominates, as it has been shown in various transport situations through porous media [3,25], the interactions of the molecules with the pore walls play the crucial role and the intermolecular collisions can be neglected. In this case, the molecules perform a series of free flights and change the flight direction independently from each other after collisions with the pore walls, as shown in Fig. 1. Therefore, the problem is reduced to many independent individual flights. In this work, we concentrate on Knudsen diffusion under Lambert's reflexion law in three-dimensional regular and irregular pores [4,11,12,15]. In this picture, the particle is absorbed from the wall after collision and after a very short time (that

TABLE I. Table of the geometries and the analytical results of the simple units from Fig. 2. Upper half: lattice systems; lower half: pores. All units are the same as in Table II.

Fig.	Sym.	ℓ_x	ℓ_y	$\ell_{x,2}$	$\ell_{y,2}$	d	$V_{x,1}$	V	D/D_0, Eq.
2(b), 6(a)	● (black)	400	19				800	838	0.91, (4)
2(b), 6(a)	▲ (blue)	200	49				400	498	0.65, (4)
2(c), 6(a)	■ (red)	10	5	4	4	1	10	32	0.31, (3)
2(e), 6(b)	● (black)	400	20				798	836	0.91, (4)
2(e), 6(b)	▲ (blue)	200	50				398	496	0.64, (4)
2(f), 6(b)	■ (red)	20	9	3	3	1	20	61	0.33, (3)

TABLE II. Table of the geometries and analytical results based of the combined systems of several building blocks from Fig. 3. Upper half: lattice systems; lower half: pores. All lengths on lattices and in pores are given in units of the lattice constant a and the pore diameter h, respectively. D is referred to the value $D_0=a^2/(4\tau)$ for the lattice ($d=2$) and to $D_0=0.37hv_0$ for the pores. All omitted numbers are equal to 1.

Figs.	Sym.	ℓ_x	ℓ_y	$\ell_{x,2}$	$\ell_{y,2}$	$V_{x,1}$	V_C	$V_{x,2}$	V	D/D_0, Eq.
3(a), 7(a)	○ (black)	200	19	200	1	400	438		638	0.57, (6)
3(a), 7(a)	★ (red)	200	49	200	1	400	498		698	0.46, (6)
3(a), 7(a)	● (blue)	200	89	200	1	400	578		778	0.36, (6)
3(b), 7(a)	□ (black)	200	59	98	9	400	498	398	953	0.75, (7)
3(c), 7(a)	◇ (black)	20	20	10	10	30	70	30	98	0.44, (7)
3(c), 7(a)	♦ (red)	20	20	20	10	40	80	40	118	0.51, (7)
3(d), 7(a)	△ (black)	20	20		10	40	98/78[a]	40	176	0.21, (8)
3(d), 7(a)	▲ (red)	10	10		10	40	80/60[a]	40	136	0.35, (8)
3(e), 7(b)	○ (black)	200	20	200		398	438		639	0.57, (6)
3(e), 7(b)	★ (red)	200	50	200		398	496		699	0.46, (6)
3(e), 7(b)	● (blue)	200	90	200		398	576		779	0.35, (6)
3(f), 7(b)	□ (black)	200	20		10	398	436	400	874	0.87, (7)
3(g), 7(b)	♦ (blue)	200	6		14	399	435	397	832	0.92, (7)
3(h), 7(b)	▲ (red)	200	21		19	400	467/437[a]	400	904	0.78, (8)

[a] $V_{c,1}$, $V_{c,2}$.

is neglected) re-emitted into a random direction, where the new direction $\vartheta \in [-\pi/2, \pi/2]$ to the normal component of the surface occurs with probability $dP(\vartheta,\varphi) \sim \cos\vartheta d\Omega$, where $d\Omega = \sin\vartheta d\vartheta d\varphi$ in $d=3$.

It is clear that disorder slows down the diffusion process, leading to a smaller value of D as compared to D_0 of a smooth system. Quantitative calculations that connect D/D_0 to simple geometrical properties, as volumes and lengths of the different segments exist for loopless curved geometries and for systems with dead ends (dangling bonds) that are connected to the main channel by a thin entry, examples of which are both shown in Fig. 2.

In loopless curved geometries [17] [see Figs. 2(b) and 2(e)], the effective length ℓ (also called "chemical length" [23,24]) of the path a particle has to travel in order to come from A to B is larger than the x distance between the same points (see Fig. 4 for an illustration). Therefore, normal diffusion with $\langle \ell^2(t)\rangle = D_0 t$ applies for the effective length and with the relation $\langle x(t)^2\rangle = (x/\ell)^2 \langle \ell(t)^2\rangle$ between x and ℓ space, one finds $D = D_0(x/\ell)^2 = D_0(V_x/V)^2$ [17], where the last expressions refer to pores with V_x and V, as defined below. In dead-end geometries [see Figs. 2(c) and 2(f)], as it was first discussed in [26], the walker only proceeds in the x channels (indicated by the red dashed lines in Fig. 2), while the time inside the dead ends increases the total time t of the walk without increasing $\langle x^2\rangle$. Quantitative considerations [18,19,22] show that $D/D_0 = V_x/V$, with the volume V_x of the x channels and the system volume V (of channel plus dead ends).

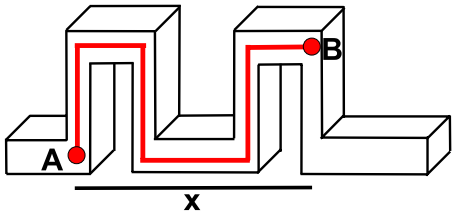

FIG. 4. (Color online) Sketch of the construction of the chemical distance ℓ between the points A and B for the curved geometry. The length of the x distance x is indicated at the bottom of the figure, while ℓ is the length of the red curved line.

In this work, we want to combine these well-known systems to more complex geometries by connecting them using additional segments or by intersecting them directly with each other, thereby, forming networks. To this end, we show how a system of different subunits, where the diffusion may be (i) uncorrelated (as in a straight channel), (ii) strongly correlated (as in dead ends, where each jump is compensated by a jump into the opposite direction), and (iii) intermediately correlated (as in curved channels, where correlated forward-backward jumps occur at all times) must be combined to obtain D/D_0 and thus κ. The approach uses the self-diffusion picture but clearly, as the self-diffusion and transport diffusion coefficients of a given geometry are equal, is also valid for transport diffusion.

III. CALCULATION OF THE DIFFUSION COEFFICIENT

A. General considerations

Generally, we can write $\langle x^2(t)\rangle$ after N time steps as

$$\langle x^2(t)\rangle = \left\langle \left(\sum_{i=1}^{N} \xi_i \right)^2 \right\rangle = \left\langle \sum_{i=1}^{N} \xi_i^2 \right\rangle + \left\langle 2 \sum_{i,j>i}^{N} \xi_i \xi_j \right\rangle, \quad (2)$$

where ξ_i and ξ_j are the single jump lengths in x direction. In the following, we call the first term of the right-hand side of Eq. (2) the "quadratic term" and the second term the "correlation term."

To calculate D directly from the geometry of the system, we refer to the well-known principles that (i) the particle concentration (as well as the gas pressure) is identical all over the system and (ii) correlations among different walks do not exist (Knudsen condition). Condition (i) tells us that in the average over many walks, all places of the system are visited with equal probability. This is true for real experiments as well as for computer simulations, provided that the starting point is chosen with equal probability among all sites.

As the sequential order of the single time steps does not play a role for evaluating the quadratic term of Eq. (2), the single steps of the sum, even if they belong to different walks, may be interchanged. Then, we can replace the time average of the quadratic term by the ensemble average and describe it solely by all jumps that occur at the same time on all places, i.e., by the geometric properties of the system and independently of the track of the single walks. We thus replace the quadratic term by $\langle \Sigma_{i=1}^{N} \xi_i^2 \rangle = N \langle \xi^2 \rangle$, where $\langle \xi^2 \rangle$ is the mean quadratic jump length in x direction over all N jumps. The total time of the walk is $t = N\langle t \rangle$, with the average duration of the time steps $\langle t \rangle$. Jumps into the y and z directions count as waiting times, as they increase t without increasing x.

On lattices, all time steps are equal and $\langle t \rangle = \tau$, whereas $\langle \xi^2 \rangle$ depends on the number of waiting times. For the diffusion coefficient D_0 of a d-dimensional ordered lattice of lattice constant a (where the correlation term is zero), we find $\langle \xi^2 \rangle = a^2/d$ and therefore $D_0 = a^2/(2d\tau)$. On a disordered lattice, on the other hand, some jump trials into the x direction find no bond and lead to additional waiting times. Furthermore, the correlation terms may give an additional negative contribution and, accordingly, $D < D_0$.

In pores, the jump lengths and time steps are not constant and therefore D_0 depends on the cross section of the pore. For the smooth pore with square surface section of side length h [see Fig. 2(d)], $D_0 = \langle \xi^2 \rangle / (2\langle t \rangle)$ is numerically found as $\approx 0.37 h v_0$, with the velocity v_0 of the particle along the trajectory (see also [12]) and with h as unit length. (The time steps can be defined as $\tau = h/v_0$). The generalization to circular or rectangular cross sections is straightforward but not the purpose of the present work. Therefore, we refer all values of D in pores to the value D_0 of the corresponding smooth pore with unit length h of Fig. 2(f) that we use as the basic element. Smooth pores with side length $n_k h$ possess the diffusion coefficient $n_k D_0$.

B. Building-block principle

We now turn to more complex geometries. The first step for a rigorous treatment is the decomposition of the considered system into well-known analytically treatable subunits k as, e.g., A: smooth x channels, B: loopless curved units, C: dead ends, and D: vertical links. The subunits must be chosen without cross correlations, i.e., such that the steps a walker performs in a given subunit do not influence the steps in another unit or during a second visit of the same unit.

The relative time t_k/t the particles spend in a given unit k can be expressed by $t_k/t = N_k/N = V_k/V$, with the relative number of sites N_k/N (in lattices) or the relative volume V_k/V (in pores) of the kth unit. We also need the relative time the particles spend in the x channels (indicated by the red dashed lines in Figs. 2 and 3), $t_{x,k}/t = N_{x,k}/N = V_{x,k}/V$, where $N_{x,k}$ and $V_{x,k}$ are the number of sites and the volume of the x channels of the kth unit, respectively. Dead ends, even if oriented in x direction, do not count as x channels. In the absence of cross correlations between the different units, $\langle x(t)^2 \rangle$ can be gained from Eq. (2) by the sum over all quadratic terms and correlation terms of all units k. As the mean quadratic jump length $\langle \xi^2 \rangle_k$ of the kth unit normally grows quadratically with the pore thickness $n_k h$ (except for possible cut-off effects in the jump-length distribution, see below) we have $\langle \xi^2 \rangle_k = n_k^2 \langle \xi^2 \rangle$ and get for the quadratic terms with $t = N\langle t \rangle$

$$\sum_i \frac{\xi_i^2}{2t} = \sum_k \frac{N_{x,k}\langle \xi^2 \rangle_k}{2N\langle t \rangle} = \sum_k n_k D_0 \frac{N_{x,k}}{N} = \sum_k n_k D_0 \frac{V_{x,k}}{V}, \quad (3)$$

where the index i runs over the time steps and k runs over the geometric subunits. For simplicity, we investigate networks with units of identical thickness here, i.e., all $n_k = 1$. If all correlation terms of all units are equal to zero, as, e.g., for a system of parallel pores, D/D_0 can be gained from Eq. (3). Otherwise, we also have to calculate the correlation terms of Eq. (2), which can be done analytically for several types of building blocks. Here, we treat the following cases:

(A) The simplest units are regular ordered lattices and straight channels [see Figs. 2(a) and 2(d)], where each jump is followed by a positive or a negative x jump with equal probability. It is common knowledge that the correlation terms of these subunits are 0.

(B) "Curved geometries" [see Figs. 2(b) and 2(e)] consist of one loopless curved backbone, where the particles perform a large number of forward-backward jumps before they pass the corners. So, the x jumps are correlated because positive x jumps to corner sites are more likely followed by negative (than by other positive) x jumps. As described above, D can be calculated by considering the problem in ℓ space, where ℓ_k is the effective or chemical length of the curve k. So, if the kth unit is a loopless curve, D of this unit alone can be written as [17]

$$D = D_0 \left(\frac{x_k}{\ell_k} \right)^2 = D_0 \left(\frac{V_{x,k}}{V_k} \right)^2, \quad (4)$$

where for the case of pores, ℓ_k and x_k have been replaced by the total volume V_k and the x volume $V_{x,k}$. From Eqs. (1)–(4), we find the correlation term of the loopless curves,

$$2 \sum_{i,j>i}^{N} \xi_i \xi_j = 2t_k \left(D - D_0 \frac{V_{x,k}}{V_k} \right) = 2t_k D_0 \left(\frac{V_{x,k}}{V_k} \right)^2 - 2t_k D_0 \frac{V_{x,k}}{V_k}, \quad (5)$$

where t_k is the total time the particle spends in k. As $V_{x,k} < V_k$, the correlation term is negative, but its absolute value is smaller than the quadratic term. So, diffusion is not suppressed, but a given jump changes the probabilities for the directions of the next jump(s) resulting in a slowing down of the diffusion.

(C) The simplest correlated subunits are dead ends [19,26], i.e., units that are connected to the other parts by a thin entry [see Figs. 2(c) and 2(f)]. The entry and the exit point to the dead ends coincide or otherwise speaking, the whole path inside the dead ends is considered as pure delay. This means that the correlation term cancels with the quadratic term, so that here, the diffusion is suppressed and both terms can be set to zero (even if, strictly speaking, none of them is zero, but one term has the negative value of the other).

(D) In straight z or y paths ("vertical links"), x jumps are not possible and, therefore, the quadratic as well as the correlation term are both equal to zero. Vertical links only increase t without increasing x and therefore act in the same way as dead ends. Indeed, these paths need not even be completely straight—it is sufficient if the lower and the upper entrance points possess the same x value.

We now turn to complex systems that can be considered as combinations of the described systems. We discuss in which way the subunits (A)–(D) can be combined without generating cross correlations between them, so that the combined geometries can be simply treated by summing over all quadratic and all correlation terms of all blocks.

(i) Dead ends (C) can be added to all systems at arbitrary positions [see Figs. 3(a) and 3(e)]. As we have seen, they do not bring new terms, but increase t. (ii) Several infinite units, e.g., (A) and (B), can be connected by vertical links (D) to form a simple network of interconnected parallel pores [see Figs. 3(b) and 3(f)]. There are no cross correlations between (A) and (B) as long as both are infinitely elongated into the x direction: if a random walker changes from (A) to (B) (or vice versa) it can continue its path in (B) into both directions with equal probability, so that no step in (A) influences later steps in (B) and vice versa. Also x correlations between (A) and (D) [or(B) and (D)] cannot exist, as x jumps in (D) either do not exist (if the link is completely straight) or exist in pairs, where positive and negative steps always cancel. Therefore, terms $\langle x_i x_j \rangle$ with x_i or x_j in (C) are either zero or appear with a negative counterpart. So, also systems of several units (A) and/or (B) connected by vertical links can be calculated by the building-block principle. (iii) A more complex combination appears, when two infinite units (A) and (B) are intersected without intermediate pieces, as shown in Figs. 3(c), 3(d), 3(g), and 3(h). Again, no cross correlations between (A) and (B) take place (by the same argument as before) and the total system can again be treated by the building-block principle. (iv) Unfortunately, not treatable this way are structures, as shown in Fig. 5(a) involving finite pieces creating short cuts inside the same structure (B), because in those cases new correlations are created [inside (B) as well as between the finite units]. (v) Also nontreatable in this way are systems where the connection between two subunits contains finite x paths, i.e., where the lower and the upper entry points do not have the same x value [see Fig. 5(b)], because in those cases cross correlations between the different finite units take place. We would like to point out, however, that in both cases new subunits could be defined, calculated numerically, and then combined with the analytical results of other exactly treatable building blocks. But this goes beyond the purpose of the present paper.

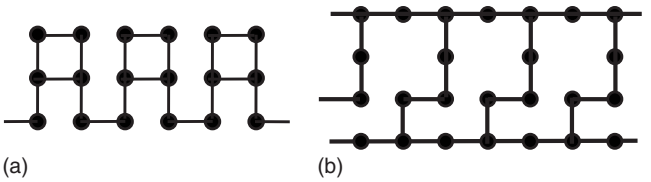

FIG. 5. Geometries (shown here as lattices) that cannot be treated by decomposing them into the building blocks (A)–(D) without cross correlations between them: (a) curve with finite connections between itself; (b) system, where two possible building blocks are interconnected by steplike units containing finite horizontal pieces.

In summary, there is a large variety of combinations of well-known building blocks, leading to quite complex geometries, from which D/D_0 can be calculated analytically, which we will show in detail in Sec. IV and verify by numerical simulations. The method is equally applicable to random walks on lattices and to diffusion in pores.

C. Numerical calculations

The analytical calculations (explained in the next section) are compared to numerical simulations on the systems shown in Figs. 2 and 3. The particle flow takes place along the x direction and the figures of the geometries are meant to be infinitely elongated along the x axis. The simulations have been performed for different geometric details (as listed in the tables) and 100–1000 elementary units have been sticked together. For technical reasons, namely, for a faster generation of the systems in the computer simulations and for the presentation of the results in tables, the systems are periodic, but all calculations are valid for completely disordered structures as well. In order to choose the starting point among all lattice sites with equal probability, periodic boundaries should be chosen in nonperiodic systems to enable walks of arbitrary length to both sides of the starting point. In the periodic systems calculated here, it is sufficient to choose the starting point with equal probability among all sites of one unit.

The computation of the random walk on a lattice is well known, so that we refer to the literature (see, e.g., [23,24]). For the diffusion processes through pores, all walls of a given geometry have been stored and ordered according to their position and orientation (normal vector $\vec{n}$). For the computations of the particle flights from wall to wall with a given direction, the possible intersections of the flight trajectory with walls of increasing distance from the particle position have been computed. Once an intersection point is found, the computation can be stopped for all walls of the same $\vec{n}$ but with larger distance to the actual particle position. The computation of $\langle x^2(t) \rangle$, once the collision point with the next wall has been found, is straightforward and takes place as on a lattice.

Note that for the subunit of the curved systems [Fig. 2(e)], some specialties exist in pores (as compared to lattices) that we mention briefly. First, due to Lambert's reflexion law, the probability for long jumps into the x direction is slightly different when starting on a vertical and on a horizontal wall,

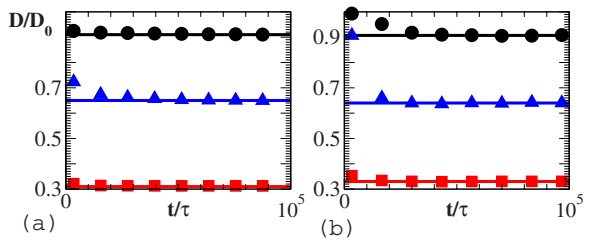

FIG. 6. (Color online) The numerical values of D/D_0 (symbols) of some simple units are plotted versus t/τ and compared to the theoretical values (straight lines) for (a) different lattice geometries [see Figs. 2(a)–2(d)] and (b) the corresponding pores [see Figs. 2(e)–2(g)] of different lengths of the segments. For the symbols and the geometric details, see Table I.

which should influence the results of rough systems slightly. However, in three-dimensional pores, these differences are not large, so that we neglect them here. (They would be more important in $2d$ pores; see Ref. [11].). Second, finite x segments lead to an upper cutoff of the jump lengths distribution $P(\xi_i)$ and therefore to a modified value of $\langle \xi^2 \rangle_k$ that cannot be taken into account analytically. Clearly, the correct jump-length distribution could be determined numerically for each system, but this is not the aim of the present work. Therefore, we choose systems with lengths of the x segments larger than the average jump length of the smooth system, so that both distributions $P(\xi_i)$ are nearly the same. The other segments (oriented along the y or z direction) may be of arbitrary lengths because there, the cutoff of the jump lengths leads to additional factors in the relation $\langle \ell^2(t) \rangle = D_0 t$ and Eq. (4) that cancel.

We test the numerical calculations on the simple units of Fig. 2, i.e., on one smooth system, one system with dead ends and one curved system and compare them to Eqs. (3) and (4), respectively. The results are shown in Fig. 6 for lattices and pores and agree perfectly with the expectations.

IV. NETWORKS OF DIFFERENT BUILDING BLOCKS

In this section, we apply the building-block principle to the geometries of Fig. 3. To this end, we need for each subunit k the number of sites N_k or the volume V_k (for lattices and pores, respectively) as well as the number $N_{x,k}$ or the volume $V_{x,k}$ of the x channels (red dashed lines in Fig. 3, see also above). Clearly, for the total system $V = \Sigma_k V_k$ and $V_x = \Sigma_k V_{x,k}$ applies.

As a first example, we consider a curved system with additional dead ends [see Figs. 3(a) and 3(e)]. In this case, the total system consists of two units $k=1$ (curve) and $k=2$ (dead ends) with the x volumes $V_{x,1} \equiv V_{x,C}$, $V_{x,2}=0$, the volumes $V_1 \equiv V_C$, $V_2 \equiv V_d$, and the total volume $V = V_C + V_d$. As described, the contributions of the dead ends cancel, so that we obtain D/D_0 by adding the quadratic term (3) and the correlation term (5) of V_C, yielding with Eq. (1), $n_k=1$ and $t_k/t = V_k/V$,

$$D = \frac{\sum_i \xi_i^2}{2t} + \frac{\sum_{i,j>i} \xi_i \xi_j}{t} = D_0 \frac{V_{x,C}^2}{V V_C}. \tag{6}$$

As a second example, we consider the curved system in parallel with a channel [see Figs. 3(b) and 3(f)], to which it is connected by additional thin vertical links. This time, the system is composed of three subunits $k=1$ (curve), $k=2$ (channel), and $k=3$ (links) with the x volumes $V_{x,1} \equiv V_{x,C}$, $V_{x,2} \equiv V_{x,Ch}$, $V_{x,3}=0$, the volumes $V_1 = V_C$, $V_2 = V_{x,2} = V_{x,Ch}$, $V_3 \equiv V_l$, and $V_x = V_{x,C} + V_{x,Ch}$, $V = V_C + V_{Ch} + V_l$. With both quadratic terms [Eq. (3)], the correlations term of Eq. (5), $n_k = 1$ and $t_k/t = V_k/V$, we find

$$D = D_0 \frac{V_{x,Ch}}{V} + D_0 \frac{V_{x,C}^2}{V V_C}. \tag{7}$$

In both examples, the dead ends as well as the vertical links only enter by increasing the total system volume.

As a third example, we consider the system of Figs. 3(c) and 3(g), consisting of the same two subunits as above. But this time, instead of being connected by additional links, they intersect each other directly, resulting in a more complex configuration as before. Also this system, even if it looks very different from the one in Figs. 3(b) and 3(f), is described by Eq. (7) and the lack of additional links only influences the total volume V that is now equal to $V = V_C + V_{Ch}$.

As the last example, we intersect two curves with volumes $V_1 \equiv V_{C_1}$, $V_2 \equiv V_{C_2}$, x volumes $V_{x,1} \equiv V_{x,C_1}$, $V_{x,2} \equiv V_{x,C_2}$, and $V = V_{C_1} + V_{C_2}$, $V_x = V_{x,C_1} + V_{x,C_2}$. We get D/D_0 by adding the quadratic and the correlation terms of both systems, yielding

$$D = D_0 \frac{V_{x,C_1}^2}{V V_{C_1}} + D_0 \frac{V_{x,C_2}^2}{V V_{C_2}}. \tag{8}$$

We can see that in all described cases, the ratio D/D_0 can be directly obtained from purely geometrical data without performing numerical simulations. If we consider lattices instead of pores, all values of V, V_k, and $V_{x,k}$ have to be replaced by the respective values of N, N_k, and $N_{x,k}$.

Nevertheless, we performed numerical simulations over an average of 10^5 systems [except for the pore systems of Eqs. (7) and (8), where due to larger calculation times, an average over only 10^3 systems has been performed] to put the relations (6)–(8) to a direct test. The results of the simulations (symbols) are shown in Fig. 7 and compared to the theoretical values (straight lines) for systems of different geometrical details, as listed in Table II. The figures show the results for lattices [Fig. 7(a)] as well as for pores [Fig. 7(b)], and in all considered cases, the agreement between numerical and theoretical data is excellent. (Larger fluctuations in the pore realizations of the two last systems are due to the poorer statistics.) Clearly, also more than two units can be combined and additional dead ends can be easily included to all considered systems to increase V, i.e., the same calculation scheme can also be applied to various other geometries, including real large networks.

V. CONCLUSION AND OUTLOOK

We have presented an analytical method to calculate the tortuosity factor κ that describes the decrease in the diffusion

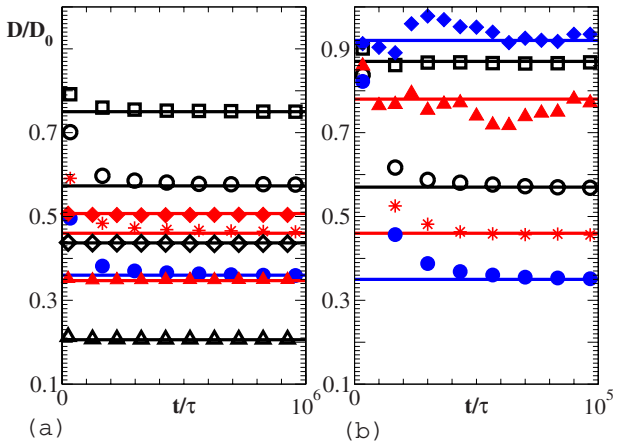

FIG. 7. (Color online) The numerical values of D/D_0 (symbols) of the systems calculated by the building-block principle are plotted versus t/τ and compared to the theoretical values (straight lines) for (a) different lattice geometries [see Figs. 2(b) and 2(c)] and (b) the corresponding pores [see Figs. 2(e) and 2(f)] of different lengths of the segments. For the symbols and the geometric details, see Table II.

coefficient D in the presence of disorder as compared to the diffusion coefficient D_0 of a smooth system for a large variety of complex disordered systems. To this end, we have developed a building-block principle that is based on a careful analysis of the correlation effects of the diffusion process. For the systems of this work, we could express κ simply by the volumes of the different substructures. The procedure has been demonstrated on many different systems and it is clear that many more systems can be constructed accordingly.

We only considered systems, where an analytical treatment is possible for both, the random walk on lattices and for the pore diffusion. However, the building-block principle can also be combined with correlations obtained from numerical simulations, as, e.g., dangling bonds with a thickness $\delta > h$ (where the correlation term does not exactly cancel with the quadratic term), curved systems where the x paths are small or backbones of varying thickness. So, additionally to the systems considered here, a large variety of pores can be manufactured and understood by combining building blocks of numerically and exactly obtained correlation terms along the lines of the present paper.

We also pointed out that not all types of combinations between subunits are suited for this treatment—if cross correlations between the subunits are created, the described method fails. We showed several examples, where this is the case. However, a large variety of quite complex systems can be treated in the way described and it is straightforward to cross, e.g., many loopless curved systems to get real networks that can be calculated by this building-block principle.

ACKNOWLEDGMENT

The author would like to thank Professor Kärger for valuable discussions.

[1] *Anomalous Transport: Foundations and Applications*, edited by R. Klages, G. Radons, and I. M. Sokolov (Wiley-VCH Verlag GmbH & Co. KGaA, Weinheim, 2008); *Adsorption and Diffusion*, edited by H. G. Karge and J. Weitkamp (Springer-Verlag, Berlin, Heidelberg, 2008).
[2] M. Felici, M. Filoche, and B. Sapoval, Phys. Rev. Lett. **92**, 068101 (2004).
[3] S. Gruener and P. Huber, Phys. Rev. Lett. **100**, 064502 (2008).
[4] J. Kärger and D. M. Ruthven, *Diffusion in Zeolites and Other Microporous Solids* (Wiley & Sons, New York, 1992).
[5] F. J. Keil, R. Krishna, and M.-O. Coppens, Rev. Chem. Eng. **16**, 71 (2000).
[6] N. Y. Chen, T. F. Degnan, and C. M. Smith, *Molecular Transport and Reaction in Zeolites* (VCH, New York, 1994).
[7] *Handbook of Porous Solids*, edited by F. Schüth, K. S. W. Sing, and J. Weitkamp (Wiley-VCH, Weinheim, 2002); J. Kärger, R. Valiullin, and S. Vasenkov, New J. Phys. **7**, 15 (2005).
[8] S. Prachayawarakorn and R. Mann, Catal. Today **128**, 88 (2007).
[9] M. P. Hollewand and L. F. Gladden, Chem. Eng. Sci. **47**, 1761 (1992).
[10] S. P. Friedman, L. Zhang, and N. S. Seaton, Transp. Porous Media **19**, 281 (1995).
[11] S. Russ, S. Zschiegner, A. Bunde, and J. Kärger, Phys. Rev. E **72**, 030101(R) (2005).
[12] S. Zschiegner, S. Russ, R. Valiullin, M.-O. Coppens, A.-J. Dammers, A. Bunde, and J. Kärger, Eur. Phys. J. Special Topics **161**, 109 (2008); S. Zschiegner, S. Russ, A. Bunde, and J. Kärger, EPL **78**, 20001 (2007).
[13] J. M. Zalc, S. C. Reyes, and E. Iglesia, Chem. Eng. Sci. **59**, 2947 (2004).
[14] S. B. Santra and B. Sapoval, Phys. Rev. E **57**, 6888 (1998).
[15] K. Malek and M.-O. Coppens, Phys. Rev. Lett. **87**, 125505 (2001).
[16] M.-O. Coppens and G. F. Froment, Fractals **3**, 807 (1995); M.-O. Coppens, Catal. Today **53**, 225 (1999); M.-O. Coppens and A. J. Dammers, Fluid Phase Equilib. **241**, 308 (2006).
[17] J. Bear, *Dynamics of Fluids in Porous Media* (Dover Publication, New York, 1988), Sec. 4.8.1.
[18] S. Revathi and V. Balakrishnan, Phys. Rev. E **47**, 916 (1993).
[19] L. Dagdug, A. M. Berezhkovskii, Y. A. Makhnovskii, and V. Y. Zitserman, J. Chem. Phys. **127**, 224712 (2007); V. Y. Zitserman, Y. A. Makhnovskii, L. Dagdug, and A. M. Berezhkovskii, Russ. J. Phys. Chem. A **82**, 2039 (2008).
[20] M. Knudsen, Ann. Phys. **28**, 75 (1909).
[21] B. Durhuus, T. Jonsson, and J. F. Wheater, J. Phys. A **39**, 1009 (2006).
[22] J.-P. Bouchaud and A. Georges, Phys. Rep. **195**, 127 (1990).
[23] *Fractals and Disordered Systems*, edited by A. Bunde and S. Havlin (Springer-Verlag, Heidelberg, 1991).
[24] D. Ben-Avraham and S. Havlin, *Diffusion and Reactions in*

Fractals and Disordered Systems (Cambridge University Press, Cambridge, 2000).
[25] M. Dvoyashkin, R. Valiullin, and J. Kärger, Phys. Rev. E **75**, 041202 (2007).
[26] R. C. Goodknight, W. A. Klikoff, Jr., and I. Fatt, J. Phys. Chem. **64**, 1162 (1960).